Microwave-Assisted Resonant Collisional Energy Transfer in Na Rydberg States

R. Kachru, N. H. Tran, and T. F. Gallagher
Molecular Physics Laboratory, SRI International, Menlo Park, California 94025
(Received 24 May 1982)

Microwave-assisted resonant collisional energy transfer process Na(ns) + Na(ns) + $h\nu$ → Na(np) + Na($(n-1)p$) is observed between two colliding Na(ns) atoms. The collisional resonance occurs when the microwave frequency ν equals the collisional energy defect $\Delta W/h$. The observed cross sections are very large ($\sim 10^8$ Å^2) and require very low microwave power, ~ 10 W/cm^2. These observations are in good agreement with an intuitive two-photon absorption model for these collisions.

PACS numbers: 32.80.-t, 32.60.+i, 42.65.Gr

Resonant collisional transfer of internal energy between two atomic or molecular species, the process in which one atom A gains the internal energy lost by the other atom B, has long attracted considerable interest. Two new approaches to this problem have recently emerged. The first employs either the term progression in a Rydberg series[1,2] or the electric field tuning of the Rydberg levels as a means of matching the transition energies of the two species. For example, the electric field tuning of Na Rydberg states was recently used to bring about the resonant process $ns + ns \rightarrow np + (n-1)p$ between two Na ns atoms which occurs when the $(n-1)p$ and np levels are Stark shifted to lie equidistant below and above the ns state. This process provides a large resonant collision cross section ($\sim 10^9$ Å^2) and narrow resonance linewidth ($\sim$1 GHz) because of the large dipole-dipole interaction between such atoms.[3,4] The second approach, frequently called radiative collision, used an external photon from an intense laser field to resonantly enhance the collisional transfer of energy.[5-7]

Here we report the use of a microwave field to resonantly enhance the collisional energy transfer between two Na Rydberg atoms, when the collisional energy defect ΔW is nonzero. We obtain large collision cross sections (peak value $\sim 10^8$ Å^2) and narrow linewidth ($\sim$1 GHz) at very low microwave powers (3–5 W) by exploiting the large dipole moments of the Rydberg states and the long dipole-dipole interaction time ($\sim$3 ns for $n = 22$). Specifically, we observe the following: In the absence of microwave field, we observe the now familiar resonant transfer of energy from the initially populated 22s states to the 21p and 22p states when the electric field is tuned so that $\Delta W = 0$. In presence of a microwave field of angular frequency ω, additional large transfer of population from the initially excited 22s states to 21p and 22p states occurs at those electric field tunings satisfying the condition $\Delta W = \pm h\omega$. It is significant to note here that the collisional energy defect ΔW can be increased or decreased arbitrarily by merely changing the dc electric field ($\sim$100 V/cm) and thereby Stark shifting the energy levels. Although the microwave-assisted collisional energy transfer (MACET) for the Rydberg states reported here is similar, in principle, to the laser-assisted collisions investigated previously,[8-10] it offers some unique possibilities not afforded by the experiments of the latter type. For instance, the cross section for MACET resonance is $\sim 10^8$ Å^2, which is 10^5 times larger than the largest observed cross section for the laser-assisted collisions.[11] Typically, several megawatts per square centimeter of laser intensity are required to observe the laser-assisted collisions, whereas the large dipole moments of the Rydberg states reduce the power requirement to $\sim$10 W/cm^2. Perhaps the most significant advantage afforded by the present experiment is the ability to change the energy defect ΔW.

The relevant energy levels for the two atoms, shown in Fig. 1, are $|1A\rangle = ns$ and $|2A\rangle = np$ for atom A, and $|1B\rangle = ns$, and $|2B\rangle = (n-1)p$ for atom B. In addition to the microwave field, a third level, as shown in Fig. 1, is required, so that

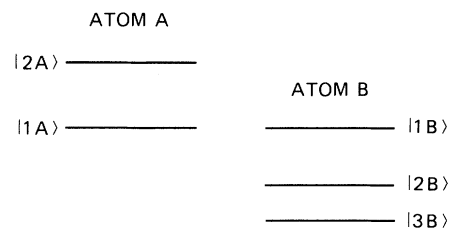

FIG. 1. Energy level diagram of the Rydberg atoms, relevant to the microwave-assisted collisions and the resonant collisions (the level $|3B\rangle$ is irrelevant for resonant collisions).

atom B may be viewed as making a two-photon transition from the initial state $|1B\rangle$ to the final state $|3B\rangle$ via the virtual intermediate state $|2B\rangle$. The first step of this two-photon transition of atom B is driven by the dipolar field of atom A,

$$E_1 \cong (\mu_1/R^3)\cos([W_{np} - W_{ns}]t/\hbar),$$

where R is the distance between the atoms, while the final step is driven by the external microwave field. At resonance, i.e., $\Delta W = \pm\hbar\omega$, the amplitude $A(b)$ of the two-photon transition from $|1B\rangle$ to $|3B\rangle$ in atom B for impact parameter b is given for low microwave powers by

$$A(b) = 2\mu_1\mu_2\mu_3 E_{MW}/h^2 b^2 V\Delta W, \quad (1)$$

where the dipole matrix elements are given by $\mu_1 = \langle 1A|\mu|2A\rangle$, $\mu_2 = \langle 1B|\mu|2B\rangle$, $\mu_3 = \langle 2B|\mu|3B\rangle$, E_{MW} is the microwave electric field amplitude, and V is the relative speed of the atoms. A classical path calculation utilizing the second-order perturbation theory is used to derive Eq. (1). ΔW is the energy mismatch of the real and virtual intermediate states shown in Fig. 1. The lowest state $|3B\rangle$ of the second atom B can in principle be any state that has a nonzero dipole matrix element connecting it to $(n-1)p$. In the present experiment, this state is the small admixture of the s and d states introduced into the $21p$ state by the Stark mixing of the levels. Although such an admixture may at first seem small, it nevertheless produces a significant dipole matrix element μ_3 (see below). Note that because of Stark mixing, the $21p$ state serves as $|2B\rangle$ and $|3B\rangle$. For low microwave powers, the major contribution to the microwave-assisted collision cross section σ_{MW} comes from impact parameters $b > b_0$.[12] In this limit the cross section is given by

$$\sigma_{MW} = (2\pi/h^4)(\mu_1\mu_2\mu_3 E_{MW}/\Delta W b_0 V)^2. \quad (2)$$

The result in Eq. (2) is similar to that derived for the laser-assisted collisions.[13-15] We note that since $\sigma_{MW} \sim \mu_1\mu_2\mu_3$, the cross sections are intrinsically large for the Rydberg states where $\mu \sim n^{*2}$. For $n = 22$, $\mu_1 = \mu_2 = 256$ a.u., whereas the dipole moments for the low excited states used in the laser-assisted collisions are ~2–3 a.u. We obtain, for microwave frequency of ~15 GHz, $\sigma_{MW} \cong 10^7$ Å^2 W^{-1}, where we have used the calculated value of 50 a.u. for μ_3, $b_0 \cong 3\times10^{-5}$ cm, and $V \cong 10^5$ cm/s. The cross section σ_{MW} at the modest power of 5 W is therefore ~10^8 Å^2, which is in excellent agreement with that observed in this experiment.

The experimental arrangement consists of an effusive Na beam which passes between a plate and a grid, where it is crossed by two collinear dye laser beams at right angles. Two Nd:(yttrium aluminum garnet)-pumped dye lasers produce 5-ns long pulses with typical energies of 150 μJ (per pulse). The first dye laser beam pumps the $3s$-$3p_{3/2}$ ($\lambda = 5890$ Å) transition of Na, while the second dye laser beam pumps the $3p_{3/2}$-ns ($\lambda = 4180$ Å) transition. Electric field tuning of the levels is achieved by applying a variable dc voltage to the lower field plate. A sweep oscillator (HP model 8690B) is used as a source of microwave (MW) field with frequency range from 12.4 to 18.0 GHz. The microwaves are amplified to power levels up to 10 W by a wide-band traveling-wave tube (TWT) (Hughes model 1477H) and are propagated into the interaction region through a glass flange with a microwave horn. A 0.3-μs rise-time electric field pulse applied 1.0 μs after the laser pulses causes field ionization of the atoms in a state-selective manner and accelerates the resulting ions to an electron multiplier detector. With use of the selective field ionization (SFI) technique, it is straightforward to resolve not only the np and the ns states, which are separated by only 50 cm^{-1} at $n = 22$, but also the $|m_l| = 0$ and 1 components of the final np state.[16] To insure against any spurious MW-induced transitions from ns to other nl states while the atoms are being field ionized, the microwaves are turned off just prior to the application to the SFI pulse. To detect the microwave-assisted collisional resonance, we scan the dc electric field rather than the microwave frequency because the parallel plate structure of our field plates does not present a constant impedance as a function of microwave frequency. Typically $\frac{1}{3}$–$\frac{1}{2}$ of the input power is coupled inside the plate region at frequencies where the MW power coupling is good.

Figure 2(a) shows the signal from the $22p$ state, observed after the excitation of the $22s$ state, as the electric field is scanned with and without a microwave field at frequency 15 GHz. In the absence of the MW field four collisional resonances are observed, as shown in Fig. 2(a) (dotted traces). Note that because of the $|m_l| = 0$ and $|m_l| = 1$ splitting of the p levels, there are four resonances, which are labeled by the $|m_l|$ values of the final lower and upper p states, respectively. The solid trace in Fig. 2(a) shows the effect of a few watts of 15-GHz microwaves as the dc field is scanned. Additional resonances now appear both on the low- and high-field side of the collisional resonances (the central reso-

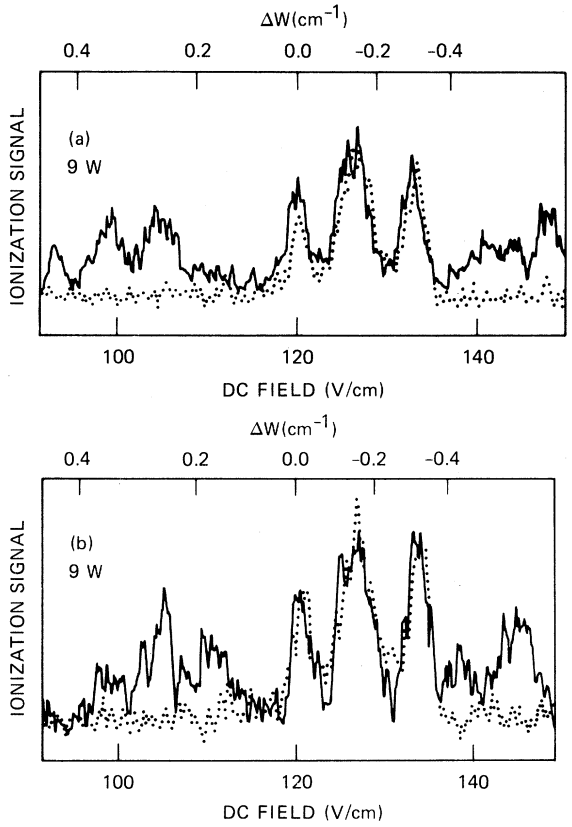

FIG. 2. The observed $22p$ ion signal after the population of $22s$ state vs the dc field in the presence of the microwave field (solid traces) of frequency (a) 15 GHz and (b) 12.4 GHz. The dotted traces were observed with no microwave field, and the sharp resonances in the center (for both solid and dotted traces) result from the resonant collisions, while the displaced resonances on sides (solid traces) are due to microwave-assisted collisions. The scale on the top of the figure is the collisional defect of the $(0,0)^+$ resonance (see text).

nances in Fig. 2). These resonances represent a large transfer of population from the initially excited $22s$ state to the $22p$ and $21p$ states. The energy defect ΔW for these additional resonances is ~15 times larger than the resonanct collision linewidth (~1 GHz). Furthermore, these resonances are clearly microwave-assisted, since no significant signal is observed (other than the resonant collision signal) in absence of MW field. The blue-laser intensity dependence of the MACET signal shows that the signal is quadratic in laser power, implying that the observed resonance is a collision signal involving two Na(ns) atoms. We label the four MW-assisted resonances according to the $|m_l|$ values of the final $(n-1)p$ and np states, respectively, i.e., as

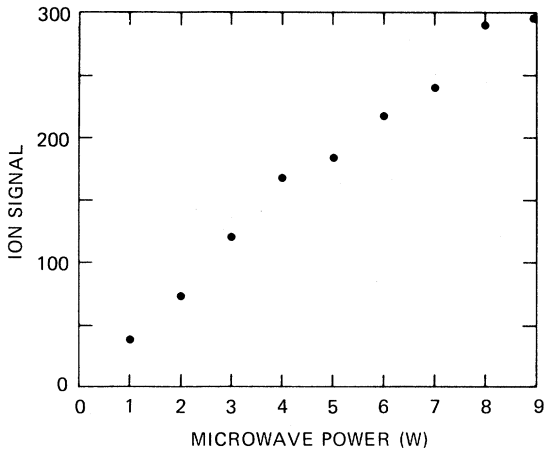

FIG. 3. The $(0,0)^+$ microwave-assisted collisional resonance signal vs the incident microwave power (at 15 GHz). Only $\frac{1}{3}$ of this power is coupled into the interaction region (see text).

$(0,0)^{\pm}$, $(1,0)^{\pm}$, $(0,1)^{\pm}$, and $(1,1)^{\pm}$ (in increasing order of the electric field), where the superscripts distinguish the microwave-assisted resonances from the resonant collision resonances; + (−) refers to $\Delta W>0$ ($\Delta W<0$). Stark-shift calculations of the Na states verify that the MACET resonance occurs (for a given microwave frequency ν) at each value of the electric field where the condition

$$|(W_{ns}-W_{np})-(W_{(n-1)p}-W_{ns})|=|\Delta W|=h\nu \qquad (3)$$

is satisfied. As shown in Fig. 2(a) the $(0,0)^+$ resonance with 15 GHz ($h\nu=0.5$ cm^{-1}) MW field occurs at ~100 V/cm as predicted by Eq. (3). Similarly, the $(0,0)^-$ resonance occurs at 140 V/cm, where $\Delta W=-0.5$ cm^{-1}. Similar agreement also holds for the other resonances. This may also be seen graphically in Fig. 2 by using the frequency scales shown at the top of Fig. 2 for the $(0,0)^+$ resonance. Figure 2(b) shows the MACET resonances at microwave frequency of 12.4 GHz and the $(0,0)^{\pm}$ resonances now appear at 0.4 cm^{-1} as predicted by Eq. (3). We estimate the MW-assisted collision cross section σ_{MW} to be $\cong\frac{1}{10}$ of that for the resonant collision,[3,4] at the highest MW power (~3 W). This means that at $n=22$, $\sigma_{MW}\cong 10^8$ Å^2. The microwave power dependence of the signal is shown in Fig. 3, where the linear dependence of the signal on the microwave power is evident. The cross section can therefore be increased to saturation by using a TWT amplifier of higher output power or by optimizing the coupling of the microwave field to the Na atoms. With a broadband coupling scheme, it is

straightforward to scan the microwave frequency at a fixed ΔW. In fact, one can easily imagine raising the power and observing the absorption of two microwave photons during the collisions.

In conclusion, we have observed microwave-assisted collisional energy transfer between two colliding Na atoms. The observed collisional resonances are continuously tunable in energy defect ΔW, and the cross sections are 10^{+5} times larger than the largest analogous cross sections for the laser-assisted collisions. The low power requirements of such collisions open a way to investigate systematically such radiatively assisted collisions.

It is a pleasure to acknowledge useful discussion with and the generous loan of the TWT amplifier by G. Tomlin. This work was supported by the U. S. Air Force Office of Scientific Research under Contract No. F49620-79-C-0212.

[1]T. F. Gallagher, G. A. Ruff, and K. A. Safinya, Phys. Rev. A 22, 843 (1980).

[2]K. A. Smith, F. G. Kellert, R. D. Rundel, F. B. Dunning, and R. F. Stebbings, Phys. Rev. Lett. 40, 1362 (1978).

[3]K. A. Safinya, J. F. Delpech, F. Gounand, W. Sandner, and T. F. Gallagher, Phys. Rev. Lett. 47, 405 (1981).

[4]T. F. Gallagher, K. A. Safinya, F. Gounand, J. F. Delpech, W. Sandner, and R. Kachru, Phys. Rev. A 25, 1905 (1982).

[5]S. E. Harris and D. B. Lidow, Phys. Rev. Lett. 33, 674 (1974).

[6]L. I. Gudzenko and S. I. Yakovlenko, Zh. Eksp. Teor. Fiz. 62, 1686 (1972) [Sov. Phys. JETP 35, 877 (1972)].

[7]S. E. Harris and J. C. White, IEEE J. Quantum Electron. 13, 972 (1977).

[8]R. W. Falcone, W. R. Green, J. C. White, J. F. Young, and S. E. Harris, Phys. Rev. A 15, 1333 (1977).

[9]Ph. Cahuzac and P. E. Toschek, Phys. Rev. Lett. 40, 1087 (1978).

[10]A. V. Hellfeld, J. Caddick, and J. Weiner, Phys. Rev. Lett. 40, 1369 (1978).

[11]W. R. Green, J. Lukaski, J. R. Willison, M. D. Wright, J. F. Young, and S. E. Harris, Phys. Rev. Lett. 42, 970 (1979).

[12]Orbiting due to the van der Waals forces between two Na(ns) atoms sets in at b_0, resulting in a decrease of radial velocity. This leads to an effective cutoff in the increase of $A(b)$ and a rapid oscillation in $A(b)$ for $b < b_0$. See S. Geltman, J. Phys. B 9, L569 (1976).

[13]Geltman, Ref. 12.

[14]P. L. Knight, J. Phys. B 10, L195 (1977).

[15]A. Gallagher and T. Holstein, Phys. Rev. A 16, 2413 (1977).

[16]T. F. Gallagher, L. M. Humphrey, W. E. Cooke, R. M. Hill, and S. A. Edelstein, Phys. Rev. A 16, 1098 (1977).

Computer Simulation of Coulomb Explosions in Doubly Charged Xe Microclusters

J. G. Gay

Physics Department, General Motors Research Laboratories, Warren, Michigan 48090

and

B. J. Berne

Department of Chemistry, Columbia University, New York, New York 10027

(Received 23 April 1982)

In recent experiments on doubly charged microclusters of Xe, no Xe_n^{++} clusters were observed for n less than 53 atoms. Computer simulations of microclusters have been carried out in which the Xe atoms interact via Lennard-Jones pair potentials and a point polarizability-dipole electrostatic model. From these simulations, it is inferred that Xe_{51}^{++} clusters have lifetimes ~100 ps while Xe_{55}^{++} clusters have lifetimes ~10 μs in agreement with the experimental result that 55-atom clusters are much more stable.

PACS numbers: 34.90.+q, 35.20.Gs, 36.40.+d, 82.20.-w

In a recent paper, Sattler *et al.*[1] have investigated the stability of charged microclusters. A polydisperse "molecular beam" of clusters of Xe, among other species, was bombarded with a low-intensity beam of electrons of sufficient energy to produce Xe^+ and Xe^{++} clusters, which were then detected by mass spectrometry. No Xe_n^{++} clusters were observed for n less than 53 atoms. The absence of small doubly charged clusters implies that Xe_n^{++} clusters consist of two Xe^+

